

defect relative to the ground state is 112 cm^{-1}). Three levels 4P in the energy region $30\,000\text{ cm}^{-1}$ are also metastable states, because optical transitions $^4P-^2S$ are forbidden in evenness and multiplicity. The Al atom can be considered as an interesting medium of r - m -lasers provided there exists a possibility of obtaining Al atoms in one of sublevels of the ground state. Optical transition from the resonant state $^2D_{3/2}$ to the metastable $^2P_{3/2}^0$ is resolved but the ratio between statistical weights of levels is not optimal.⁸

The next peculiarity of the Al atom structure is that there exist $^2D_{3/2,5/2}$ states of the configuration $3s^24p$ close to (in the energy scales) resonant states $^2P_{1/2,3/2}$. They are connected by optical transitions with the singlet level $^2S_{1/2}$ (doublet $\lambda = 1312\text{ nm}$ and 1315 nm in Fig. 1). Laser effects were observed in gas-discharge plasma at such infrared transitions in the structure of the first excited states of atoms having no evident channels of selective electron excitation of upper working states. This fact was first observed when analyzing the inversion mechanisms in the Yb atomic spectrum.^{9,10} The same laser effects were observed at infrared transitions of strontium¹¹ and thulium^{10,12} atoms as well. These observations point to the existence of a sufficiently common inversion mechanism of the first excited atomic states in the pulse electric discharges. At present, two concepts exist on possible mechanism of pumping the first excited but non-resonant atom states in the discharge plasma. One of them¹³ assumes photodissociation in a discharge of molecular components of the working mixture under the action of natural resonance radiation of atoms¹⁴; another concept means the excitation transmission from the resonance state to neighboring ones in super-elastic electron shocks in the discharge plasma.¹⁴

Thus, the above-mentioned analysis has shown that spectroscopic investigations of laser optical excitation of resonant states of the Al atom are useful for understanding phenomena taking place in metal vapor located both in the resonance radiation field and in the discharge plasma.

The experiments were conducted using a setup consisting of a tunable laser, a cell with Al vapor and a system of vapor radiation registration (Fig. 2).

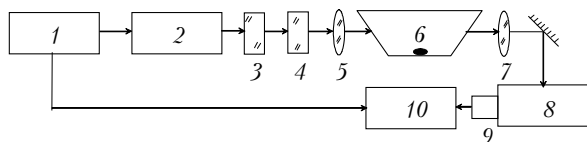


Fig. 2. Schematic representation of the experimental setup: excimer laser 1; dye laser 2; frequency doubler 3; filters 4; long-focus lenses 5, 7; cell with Al vapor 6; monochromator 8; system of photoreceivers 9; analog system of signal processing 10.

Cells of two types were used for preparation of Al vapor. In one of the cells the pieces of metal Al were placed into a ceramic tube made of pure

aluminum oxide, with an internal diameter of 1 cm and an active part length of 20 cm. As a heat insulator, the zirconium dioxide powder was used, located between the ceramic tube and external cell sheath being a quartz tube of 6.2 cm in diameter. The active area was heated to a necessary temperature by a molybdenum spiral, wound around the ceramic tube, to which the alternating current was applied. Such a construction allows heating active area up to 1500°C . A cell of this type is traditional for metal vapor laser technology.

Its major disadvantages are the presence of the insulator powder, which at high temperatures has a chemical effect on the molybdenum wire (the molybdenum wire temperature is always higher than the temperature inside the ceramic tube), and a long-time outgassing. The former limits the cell service time, the latter results in uncontrolled changes in gas composition inside the cell. The uncontrolled changes in the gas composition can also result in gaseous products arising from chemical interaction of molybdenum with the insulator powder.

A cell of the second type does not contain the zirconium dioxide powder. A system of heat screens is used in it as the heat insulator. Such a system consists of three thin-wall cylinders made of molybdenum foil and located coaxially with the ceramic tube and external quartz sheath. The cylinder diameters are 24, 42, and 54 cm, respectively. The length of all three cylinders is equal to the ceramic tube length (40 cm). Such a construction allows an existence of a uniform heating zone of 18 cm long in the central part of the cell. The increased energy consumption because of high radiation losses is a disadvantage of this construction.

The experiment involved studies of the spectrum of the resonance and quasi-resonance UV radiation scattered by Al vapor and its transformation at varying densities of vapor and buffer gas. Observations were conducted along the cell axis toward the exciting radiation.

As a rule, four lines of the superradiant emittance are observed in the scattered radiation spectrum. Two of them lay in the near infrared range at transitions shown in Fig. 1 and two are in the dark-blue range at transitions to the atom ground state. In the visible range, the superluminous emittance was determined visually using the directional diagram of the scattered radiation. For infrared lines the presence of superluminous emittance regime was determined from augmentation of the signal intensity, when placing a dielectric mirror to the $1.3\text{ }\mu\text{m}$ range between filter 4 and lens 5.

Studies of intensity distribution over the scattered signal spectrum have revealed a connection of the intensity with the exciting radiation spectrum and the buffer gas density. Figure 3 shows the symmetric behavior of intensities of the visible and infrared lines in pairs at variations of the buffer gas (helium) density.

The pair symmetry implies that at vapor excitation by radiation at $\lambda = 308\text{ nm}$ the dependence of the

396-nm intensity on the helium density is described by curve 1 (Fig. 3a), and of the 394-nm intensity – by curve 2, while at vapor excitation by 309-nm radiation the inverse intensity distribution is observed for scattered radiation, i.e., the dependences in Fig. 3a change places. The pair symmetry in behavior of intensities at growing helium density is typical of infrared lines of superradiant emittance as well. In particular, the vapor excitation by the radiation at $\lambda = 308$ nm results in excitation of superradiant emittance predominantly at $\lambda = 1312$ nm (Fig. 3b, curve 1) as compared to $\lambda = 1315$ nm (Fig. 3b, curve 2); at a change of the exciting radiation wavelength – to predominant superradiant emittance excitation at $\lambda = 1315$ nm, i.e., curves 1 and 2 change places.

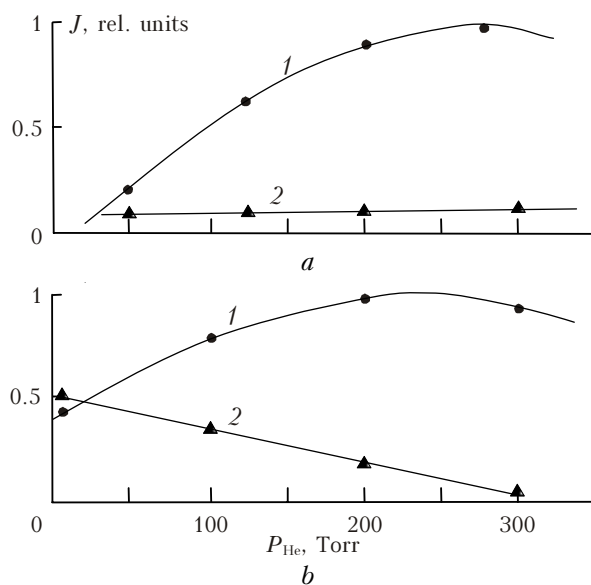


Fig. 3. Dependence of line intensities of aluminum vapor superradiant emittance on the helium density.

Dependences in Fig. 3 indicate that the buffer gas participates in the superradiant emittance at Al lines. Probably, one of mechanisms of such a participation is connected with the energy transmission from pump-excited states $^2P_{1/2,3/2}$ to the levels $^2D_{3/2,5/2}$ (energy defect is 513 cm^{-1}). It should be also taken into account that there is a common level 2S for all four observed lines, i.e., both the cascade pumping and the transition competition take place.

To reveal the role of cascade pumping in the emergence of superradiant emittance at resonance transitions, experiments were conducted with the IR cavity modulation at $\lambda = 1315$ and 1312 nm. These experiments have shown that the cascade pumping

is not a basic excitation process for $\lambda = 394$ and 396 nm lines. For superradiant emittance at these lines, an individual pumping process should take place. We believe that the dissociation of the vapor molecular component can be such process, as is shown in Fig. 4.

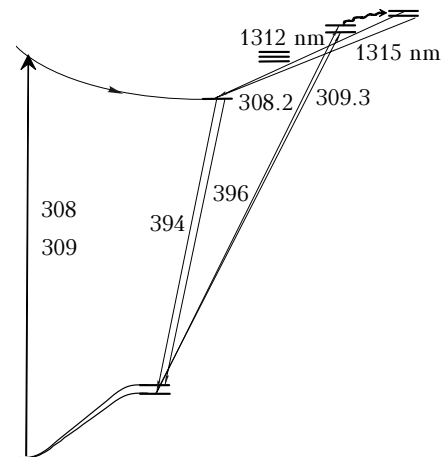


Fig. 4. Diagram of participation of molecular and atomic vapor components in formation of the scattered radiation spectrum.

References

1. B.A. Glushko, M.E. Movsesyan, and T.O. Ovakimyan, *Opt. Spektrosk.* **52**, No. 4, 762 (1982).
2. S.N. Atutov, A.I. Plekhanov, and A.M. Shalagin, *Opt. Spektrosk.* **56**, No. 4, 134 (1984).
3. Z. Konefal, *Opt. Commun.* **164**, 95–105 (1999).
4. J.J. Kim and N. Sung, *Opt. Lett.* **12**, No. 11, 885–887.
5. V.M. Klimkin, V.S. Verkhovskii, V.E. Prokopiev, V.F. Tarasenko, V.G. Sokovikov, and A.I. Fedorov, *Sov. J. Quant. Electron.* **12**, No. 11, 1397–1400 (1982).
6. V.M. Klimkin, V.E. Prokopiev, and V.G. Sokovikov, in: *Technical Digest of XIth All-Union Conf. on Coherent and Nonlinear Optics* (Erevan, 1982), Part 1, pp. 76–77.
7. V.M. Klimkin, V.N. Nikolaev, V.G. Sokovikov, and V.B. Shcheglov, *Pis'ma Zh. Eksp. Teor. Fiz.* **34**, No. 3, 111–114 (1981).
8. V.M. Klimkin, *Teplofiz. Vysokikh Temp.* **XXIII**, No. 3, 568–571 (1985).
9. V.M. Klimkin, *Sov. J. Quant. Electron.* **5**, No. 3, 326–328 (1975).
10. Ph. Cahuzac, *Phys. Lett.* **27**, No. 8, 473–474 (1968).
11. Ph. Cahuzac, *J. Phys. (Paris)* **32**, No. 7, 499–505 (1971).
12. V.A. Gerasimov and B.P. Yunzhakov, *Sov. J. Quant. Electron.* **19**, No. 12, 1532–1536 (1989).
13. V.M. Klimkin and V.G. Sokovikov, in: *Abstracts of Reports at VI Int. Conf. on Atom. Molec. Pulse Lasers* (Erevan, 2003), Part. 1, p. 25.
14. T.M. Gorbunova, A.N. Soldatov, and A.G. Filonov, *Atmos. Oceanic Opt.* **17**, Nos. 2–3, 231–234 (2004).